Research Article

Engineering: Open Access

Power XShanker Distribution: Properties, Estimation, and Applications

Franklin C. Oha[1], Harrison O. Etaga[2], Precious O. Ibeakuzie[3], Ifeanyi C. Anabike[4], and Okechukwu J. Obulezi[5]*

[1,2,3,4,5]*Department of Statistics, Faculty of Physical Sciences, Nnamdi Azikiwe University, Awka, Nigeria*

***Corresponding Author**
Okechukwu J. Obulezi, Department of Statistics, Faculty of Physical Sciences, Nnamdi Azikiwe University, Awka, Nigeria

Submitted: 2024, Dec 11; **Accepted:** 2024, Jan 19; **Published:** 2024, Jan 26

Citation: Oha, F.C., Etaga, H.O., Ibeakuzie, P.O., Anabike, I.C., Obulezi, O.J. (2024). Power XShanker Distribution: Properties, Estimation, and Applications. *Eng OA, 2*(1), 01-20.

Abstract
A two-parameter extension of the XShanker distribution called power XShanker is developed and studied in this article. The properties which include moment, quantile function, moment generating function, order statistics, stress-strength reliability function, and Rény entropy were studied. The classical and Bayesian estimation procedures were studied with simulations. The usefulness of the proposed model was demonstrated using lifetime data sets.

Keywords: Estimation, Lifetime Data, Power X Shanker Distribution, Simulation Studies, X Shanker Distribution

1 Introduction
New ideas and innovations are birthed daily in reaction to the complexities associated with life. In distribution theory, for instance, the development of new models has been on the increase for the last two decades. Most of the recent developments have been centered around intuitive modification and extension of existing models. The reasons are not far-fetched namely flexibility, tractability, parsimony, and applicability. We must remind ourselves, therefore, that a very powerful model in a given scenario might be worthless in another scenario and vice versa. Again, the goodness of fit is not the only feature of interest in modeling, model performance in terms of parameter estimation is also vital. Interest can also span into functions that are amenable to mathematical manipulations. For instance, experience has shown that distributions that possess closed-form quantile functions are less tedious in use and can easily lend themselves to simulation studies.

Power-transformed distributions enjoy applicability in data with a polynomial nature. In reality, such data are common in stock market records, biomedical events, the tensile strength of an engineering material, etc. Some of the existing articles on power-transformed Lindley-class of distributions are [1-12]. The gap in the literature is that none of these power-transformed Lindley-class creations has harnessed the estimation of parameters using the Bayesian approach. Bayesian estimation is an important creation in inference which depends on prior information about the characteristics and nature of the event of interest when making posterior computation. Many other variant models in the Lindley class are necessary to mention such as [13-15].

In this article, a concise discussion of the properties of the proposed model is done, a detailed study of the classical estimation procedures is carried out, and then the Bayesian estimation based on the linear-exponential loss, squared error loss, and generalized entropy loss functions was given adequate attention. The remainder of this work is in the following sequence. Section two dwells on the derivation of the power XShanker distribution. In section three, the essential properties which include the moment and quantile function, etc were studied. In section four, the non-Bayesian estimation was discussed and in section five, the Bayesian method of estimation was studied. Simulation studies for both classical and Bayesian estimation procedures are carried out. Applications to lifetime data are demonstrated in section seven. The article ended with concluding remarks in section eight.

2 Power XShanker Distribution
Etaga, Celestine, et al. (2023) developed the XShanker Distribution (XSD) with PDF and CDF respectively given as

$$f(x;\theta) = \frac{\theta^2}{\left(\theta^2+1\right)^2}\left(\theta^3+2\theta+x\right)e^{-\theta x}; \quad x>0, \tag{1}$$

and

$$F(x;\theta) = 1-\left\{1+\frac{\theta x}{\left(\theta^2+1\right)^2}\right\}e^{-\theta x}, \tag{2}$$

where $\theta > 0$ is the scale parameter. Using the box-muller transformation $Y = X^{\frac{1}{c}}$, for $X \sim$ XShanker (θ), where $c > 0$ is the shape parameter, the new random variable X assumes the following PDF and CDF

$$f(y;\theta,c) = \frac{c\theta^2}{\left(\theta^2+1\right)^2}\left(\theta^3+2\theta+y^c\right)y^{c-1}e^{-\theta y^c}; \quad y>0, \tag{3}$$

and

$$F(y;\theta,c) = 1-\left\{1+\frac{\theta y^c}{\left(\theta^2+1\right)^2}\right\}e^{-\theta y^c} \tag{4}$$

Eq. 3 and 4 are respectively the PDF and CDF of the Power XShanker Distribution (PXSD). Notice that PXSD reduces to the XSD when $\alpha = 1$.

The survival function $S(y) = 1-F(y;\theta,c)$ and the hazard rate function $h(y) = \frac{f(y)}{S(y)}$ of the PXSD are given as follows

$$S(y) = \left\{1+\frac{\theta y^c}{\left(\theta^2+1\right)^2}\right\}e^{-\theta y^c} \tag{5}$$

and

$$h(y) = \frac{c\theta^2\left(\theta^3+2\theta+y^c\right)y^{c-1}}{\theta^4+2\theta^2+y^c+1} \tag{6}$$

The shape of the PDF in figure 1 shows that it is a right-skewed decreasing function. The figures 2- 5 demonstrate varying shapes of the hazard rate function. It is increasing reversed L-shaped, approximately J-shaped, decreasing L-shaped, and strictly increasing shaped respectively. These characteristics lend the distribution to many applications.

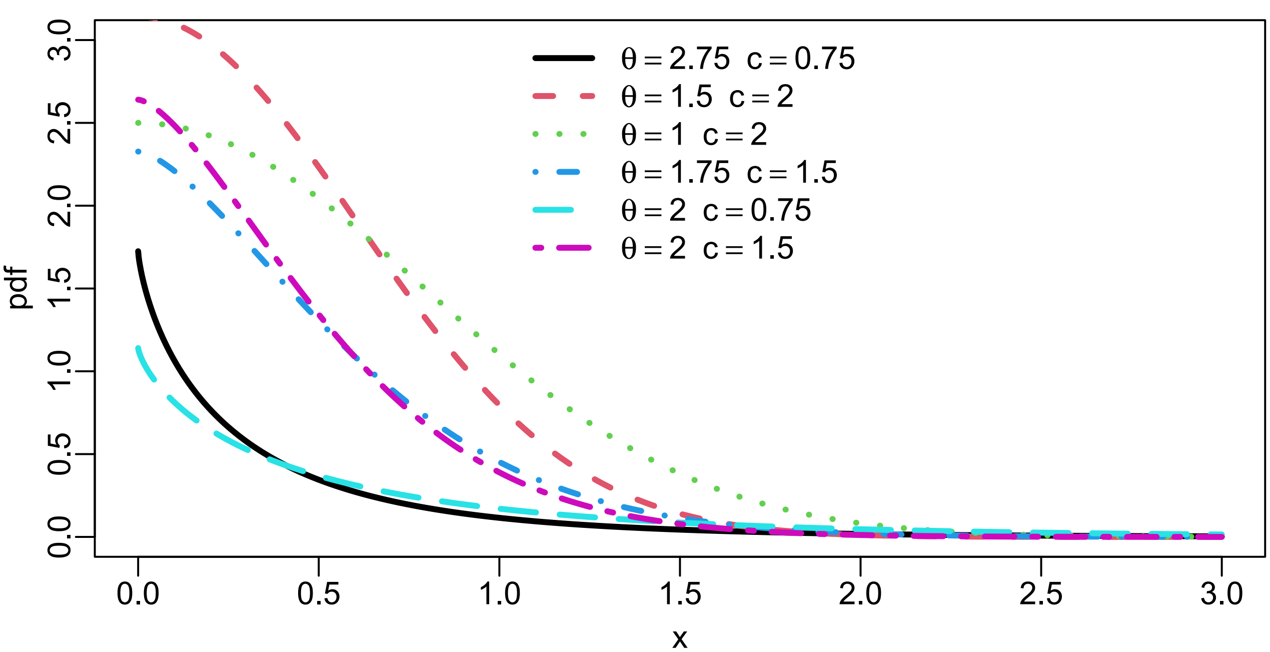

Figure 1: PDF of PXSD(θ, c)

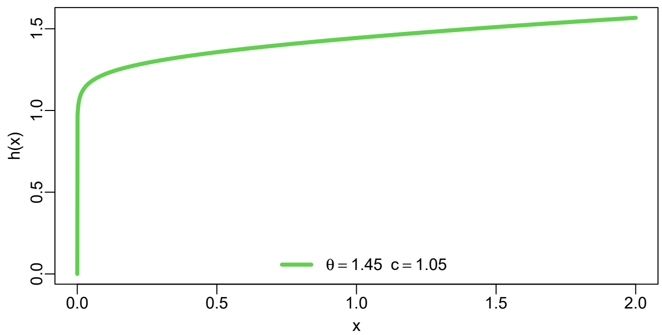

Figure 2: hazard function of PXSD(θ, c)

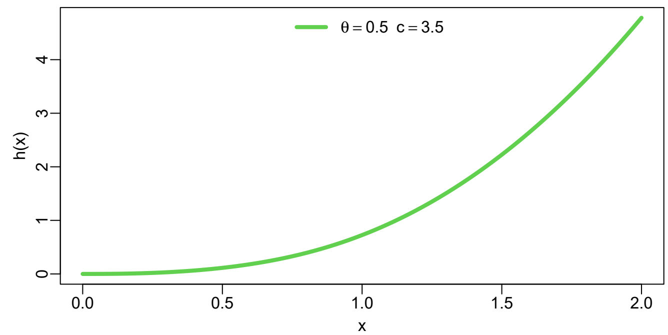

Figure 3: hazard function of PXSD(θ, c)

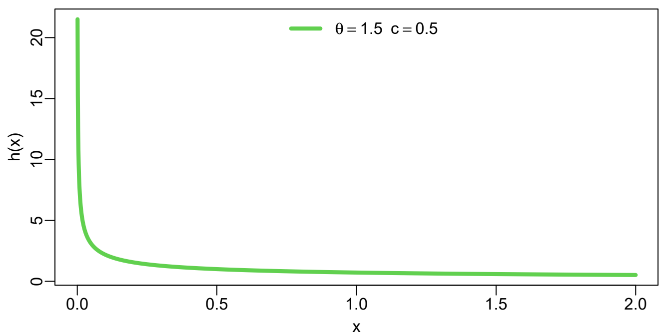

Figure 4: hazard function of PXSD(θ, c)

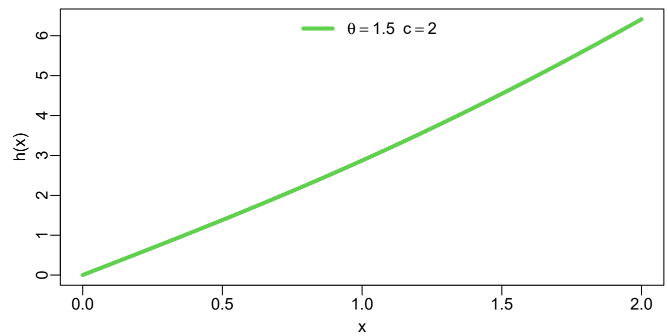

Figure 5: hazard function of PXSD(θ, c)

3 Useful Properties

In this section, we discuss some important statistical characteristics of the proposed PXSD.

3.1 Quantile Function

Let $Y \sim$ PXSD (θ, c), if the CDF in Eq. 4 is inverted such that $u \sim$ U $(0,1)$ then the quantle function is given by

$$\mathbb{Q}(u) = \left\{ \frac{-\left(\theta^2+1\right)^2 - \mathbb{W}_{-1}\left[-(1-u)(\theta^2+1)^2 e^{-(\theta^2+1)^2}\right]}{\theta} \right\}^{\frac{1}{c}} \tag{7}$$

Proof. Let replace $F(y;\theta c)$ with u in Eq. 4, so that

$$(1-u)\left(\theta^2+1\right)^2 = \left(\left(\theta^2+1\right)^2 + \theta y^c\right) e^{-\theta y^c} \tag{8}$$

If we multiply both sides by a minus sign, then let $Z(y) = -\left(\left(\theta^2+1\right)^2 + \theta y^c\right) \implies Z(y) + \left(\theta^2+1\right)^2 = -\theta y^c$. This yields

$$\begin{aligned} -(1-u)\left(\theta^2+1\right)^2 &= Z(y) e^{Z(y)+(\theta^2+1)^2} \\ -(1-u)\left(\theta^2+1\right)^2 e^{-(\theta^2+1)^2} &= Z(y) e^{Z(y)} \end{aligned} \tag{9}$$

Taking the Lambert W function, we have

$$\mathbb{W}_{-1}\left[-(1-u)(\theta^2+1)^2 e^{-(\theta^2+1)^2}\right] = Z(y) \tag{10}$$

where $Z(y) = -\left(\left(\theta^2+1\right)^2 + \theta y^c\right)$, the rest is trivial. □

3.2 Moment

The crude moment enables the computation of the mean and other measures such as variance, skewness, and kurtosis. Let $Y \sim$ PXSD (θ, c), then the rth crude moment is obtained as

$$\mu_r^{'} = \frac{c\theta^2}{\left(\theta^2+1\right)^2}\left\{\frac{\theta^3+2\theta}{\theta^{\frac{r}{c}+1}}\Gamma\left[\frac{r}{c}+1\right]\frac{1}{\theta^{\frac{r+1}{c}+1}}\Gamma\left[\frac{r+1}{c}+1\right]\right\}; \quad r = 1, 2, \cdots \tag{11}$$

Proof. The rth crude moment is defined as $\mu_r^{'} = \mathbb{E}Y^r = \int_0^\infty y^r f(y)\,dy$, where $f(y)$ represents the density function for with support $y > 0$. Replacing $f(y)$ with the PDF of PXSD gives

$$\mu_r^{'} = \int_0^\infty \frac{c\theta^2}{\left(\theta^2+1\right)^2}\left(\theta^3+2\theta+y^c\right)y^{r+c-1}e^{-\theta y^c}\,dy \tag{12}$$

This can be rewritten as

$$\mu_r^{'} = \frac{c\theta^2}{\left(\theta^2+1\right)^2}\left\{\left(\theta^3+2\theta\right)\int_0^\infty y^{r+c-1}e^{-\theta y^c}\,dy + \int_0^\infty y^{r+c}e^{-\theta y^c}\,dy\right\} \tag{13}$$

Let $t = \theta y^c \implies \left(\frac{x}{\theta}\right)^{\frac{1}{c}}$ and $dy = \frac{x^{\frac{1}{c}-1}}{c\theta^{\frac{1}{c}}}dx$, then the rest is trivial. □

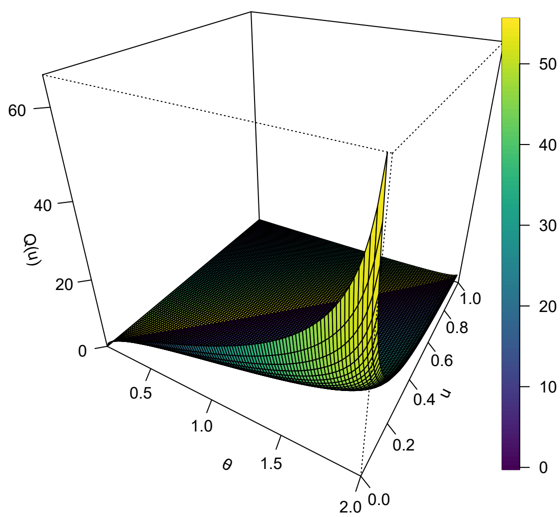

Figure 6: Q(u) of PXSD (θ, c)

Replacing r with 1 gives the mean. The variance can be obtained from the moment following $EY = EY^2 - [EY]^2$. The Bowley's skewness (η) and Moore's kurtosis (ξ) are derived from the quantile function and are respectivelgiven as;

$$\eta = \frac{\mathbb{Q}\left(\frac{3}{4}\right)+\mathbb{Q}\left(\frac{1}{4}\right)-2\mathbb{Q}\left(\frac{1}{2}\right)}{\mathbb{Q}\left(\frac{3}{4}\right)-\mathbb{Q}\left(\frac{1}{4}\right)} \tag{14}$$

and

$$\xi = \frac{\mathbb{Q}\left(\frac{7}{8}\right)-\mathbb{Q}\left(\frac{5}{8}\right)+\mathbb{Q}\left(\frac{3}{8}\right)-\mathbb{Q}\left(\frac{1}{8}\right)}{\mathbb{Q}\left(\frac{3}{4}\right)-\mathbb{Q}\left(\frac{1}{4}\right)} \tag{15}$$

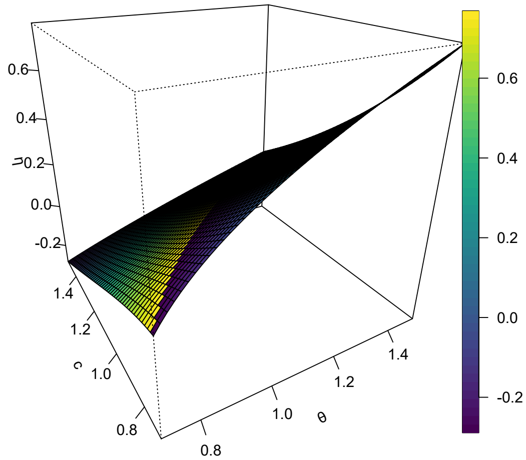

Figure 9: skewness of PXSD(θ, c)

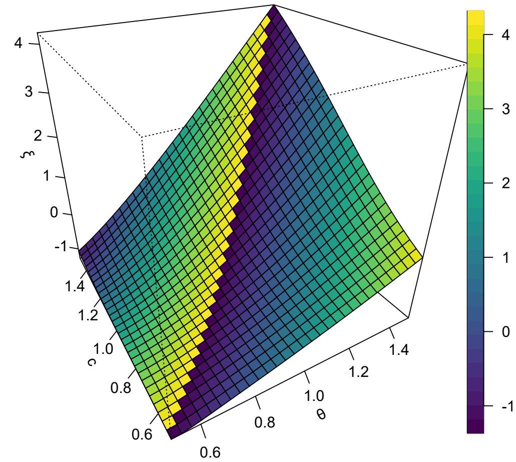

Figure 10: kurtosis of PXSD(θ, c)

The variance plot in figure 7 justifies the shape of the PDF in figure 1 that $X \sim$ PXSD (θ, c) contains a high dispersion from the mean. Figure 9 indicates that the distribution has a positive skewness. While figure 10 shows that the distribution is leptokurtic (highly peaked).

3.3 Moment Generating Function

Let $Y \sim$ PXSD (θ, c) where it exists, the moment generating function (MGF) written as $M_Y(t)$ is defined as

$$M_Y(t) = \mathbb{E}e^{ty} = \int_0^\infty e^{ty} f(y;\theta,c)\,dy = \frac{c\theta^2}{(\theta^2+1)^2} \sum_{j=0}^{\infty} \frac{(-1)^j}{j!}\theta^j \left\{ (\theta^3+2\theta)\frac{\Gamma[c(1+j)]}{(-t)^{c(1+j)}} + \frac{\Gamma[c(2+j)]}{(-t)^{c(2+j)}} \right\} \tag{16}$$

3.4 Order Statistics

Let $Y_1, Y_2, \cdots, X_n$ be the ordered statistics of a random sample $y_1, y_2, \cdots, y$ from the continuous population with PDF $f(y;\theta, c)$ and CDF $F(y;\theta, c)$ then the PDF of r^{th} order statistics Y^r is given by

$$\begin{aligned} f_{y(r)} &= \frac{n!}{(r-1)!(n-r)!} f(y)[F(y)]^{r-1}[1-F(y)]^{n-r} = \sum_{j=0}^{\infty}(-1)^j \frac{n!}{j!(r-1)!(n-r-j)!} f(y)F^{j+r-1}(y) \\ &= \sum_{i,j,k,l=0}^{\infty} \frac{(-1)^{i+j+l}}{i!} \frac{n!}{j!(n-r)!(n-r-j)!} \frac{(1+i)^l \theta^{k+l+2} y^{c(k+l+1)-1}}{(\theta^2+1)^{2(1+k)}} \binom{i}{k}\binom{j+r-1}{i} \left(\theta^3+2\theta+y^c\right) \end{aligned} \tag{17}$$

3.5 Stress-Strength Reliability Analysis

Let $y \sim$ PXSD (θ_1, c_1) and x ~ PXSD (θ_2, c_2) be the stress and strength of a system that assumes the proposed PXSD, then the reliability of PXSD can be expressed as

$$\begin{aligned} R_{\text{PXSD}} &= P(x<y) = \int_0^\infty \int_0^y f(x)f(y)\,dy\,dx \\ &= 1 - \frac{\theta_1^2}{(\theta_1^2+1)^2} \sum_{j=0}^{\infty} \frac{(-1)^j}{j!} \theta_2^j \left\{ \frac{\theta_1^3+2\theta_1}{\theta_1^{jr+\frac{1}{c_1}+1}} \Gamma\left[jr+\frac{1}{c_1}+\right] + \frac{\Gamma\left[jr+\frac{1}{c_1}+2\right]}{\theta_1^{jr+\frac{1}{c_1}+2}} \right. \\ &\quad \left. + \frac{\theta_2(\theta_1^3+2\theta_1)}{(\theta_1^2+1)^2} \frac{\Gamma\left[(j+1)r+\frac{1}{c_1}+1\right]}{\theta_1^{(j+1)r+\frac{1}{c_1}+1}} + \frac{\theta_2}{(\theta_2^2)^2} \frac{\Gamma\left[(j+1)r+\frac{1}{c_1}+2\right]}{\theta_1^{(j+1)r+\frac{1}{c_1}+2}} \right\}; \quad \text{where} \quad r = \frac{c_2}{c_1} \end{aligned} \tag{18}$$

Proof.

$$R = P(x<y) = \int_0^\infty \int_0^y f(x)f(y)\,dy dx = \int_0^\infty f(y)F(y)\,dy \tag{19}$$

Plugging in Eq. 3 and 4, we have

$$\begin{aligned} R_{\text{PXSD}} = 1 - \frac{c_1\theta_1^2}{\left(\theta_1^2+1\right)^2}\sum_{j=0}^{\infty}\frac{(-1)^j}{j!}\theta_2^j\Bigg\{\left(\theta_1^3+2\theta_1\right)\int\limits_0^\infty y^{jc_2+c_1}e^{-\theta_1 y^{c_1}}\,dy + \int\limits_0^\infty y^{jc_2+2c_1}e^{-\theta_1 y^{c_1}}\,dy \\ + \frac{\theta_2\left(\theta_1^3+2\theta_1\right)}{\left(\theta_2^2+1\right)^2}\int\limits_0^\infty y^{jc_2+c_1+c_2}e^{-\theta_1 y^{c_1}}\,dy + \frac{\theta_2}{\left(\theta_2^2+1\right)^2}\int\limits_0^\infty y^{jc_2+2c_1+c_2}e^{-\theta_1 y^{c_1}}\,dy\Bigg\} \end{aligned} \tag{20}$$

where $e^{-\theta_2 y^{c_2}} = \sum_{j=0}^{\infty}\frac{(-1)^j}{j!}\theta_2^j y^{jc_2}$ using power series expansion. Define $t=\theta_1 y^{c_1} \implies y = \left(\frac{t}{\theta_1}\right)^{\frac{1}{c_1}}$, and $dy = \frac{t^{\frac{1}{c_1}-1}}{c_1\theta_1^{\frac{1}{c_1}}}dt$.
Hence,

$$\begin{aligned} R = 1 - \frac{\theta_1^2}{\left(\theta_1^2+1\right)^2}\sum_{j=0}^{\infty}\frac{(-1)^j}{j!}\theta_2^j\Bigg\{\frac{\left(\theta_1^3+2\theta_1\right)}{\theta_1^{jr+\frac{1}{c_1}+1}}\int_0^\infty t^{jr+\frac{1}{c_1}}e^{-t}\,dt + \frac{1}{\theta_1^{jr+\frac{1}{c_1}+2}}\int_0^\infty t^{jr+\frac{1}{c_1}+1}e^{-t}\,dt \\ + \frac{\theta_2\left(\theta_1^3+2\theta_1\right)}{\left(\theta_2^2+1\right)^2\theta_1^{(j+1)r+\frac{1}{c_1}+1}}\int_0^\infty t^{(j+1)r+\frac{1}{c_1}}e^{-t}\,dt + \frac{\theta_2}{\left(\theta_2^2+1\right)^2\theta_1^{(j+1)r+\frac{1}{c_1}+2}}\int_0^\infty t^{(j+1)r+\frac{1}{c_1}+1}e^{-t}\,dt\Bigg\} \end{aligned} \tag{21}$$

and the rest is trivial. □

3.6 Rény Entropy

One of the common measures of entropy is the Rény entropy. It is a measure of the amount of information in the data sets. It is defined for $\omega \neq 1$ and $\omega > 0$.

Definition 3.1. Let $Y \sim$ PXSD (θ, c), then the Rény entropy R_E can be expressed as

$$R_E = \frac{1}{1-\omega}\log\left\{\frac{c^{\omega-1}\theta^{2\omega}}{\left(\theta^2+1\right)^{2\omega}}\sum_{j=0}^{\infty}\binom{\omega}{j}\left(\theta^3+2\theta\right)^{\omega-j}(\theta\omega)^{-(j-\omega-\frac{\omega}{c}+\frac{1}{c})}\Gamma\left[j-\omega-\frac{\omega}{c}+\frac{1}{c}\right]\right\} \tag{22}$$

Proof. The Rény entropy is generally defined as

$$R_E = \frac{1}{1-\omega}\log\left\{\int_0^\infty f^\omega(y;\theta,c)dy\right\} \tag{23}$$

where $f(y;\theta,c)$ is the PDF of the PXSD as defined in Eq. 3. Plug in Eq. 3, we obtain

$$R_E = \frac{1}{1-\omega}\log\left\{\int_0^\infty \frac{c^\omega\theta^{2\omega}}{\left(\theta^2+1\right)^{2\omega}}\left(\theta^3+2\omega+y^c\right)^\omega y^{(c-1)\omega}e^{-\theta\omega y^c}\,dy\right\} \tag{24}$$

Using the general binomial expansion on $\left(\theta^3+2\omega+y^c\right)^\omega$, we obtain

$$R_E = \frac{1}{1-\omega}\log\left\{\frac{c^\omega\theta^{2\omega}}{\left(\theta^2+1\right)^{2\omega}}\sum_{j=0}^{\infty}\binom{\omega}{j}\left(\theta^3+2\theta\right)^{\omega-j}\int_0^\infty y^{jc-\omega c-\omega}e^{-\theta\omega y^c}\,dy\right\} \tag{25}$$

Define $t=\theta\omega y^{c} \implies y=\left(\frac{t}{\theta\omega}\right)^{\frac{1}{c}}$ and $dy=\frac{t^{\frac{1}{c}}}{c(\theta\omega)^{\frac{1}{c}}}\,dt$. Then

$$R_E=\frac{1}{1-\omega}\log\left\{\frac{c^{\omega-1}\theta^{2\omega}}{\left(\theta^2+1\right)^{2\omega}}\sum_{j=0}^{\omega}\binom{\omega}{j}\left(\theta^3+2\omega\right)^{\omega-j}(\theta\omega)^{-(j-\omega-\frac{\omega}{c}+\frac{1}{c})}\int_0^{\infty}t^{j-\omega-\frac{\omega}{c}+\frac{1}{c}-1}e^{-t}\,dt\right\} \tag{26}$$

and the rest is trivial. □

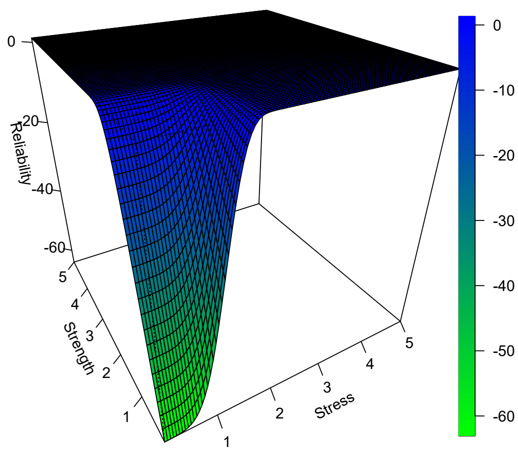

Figure 11: stress-strength reliability of PXSD(θ, c)

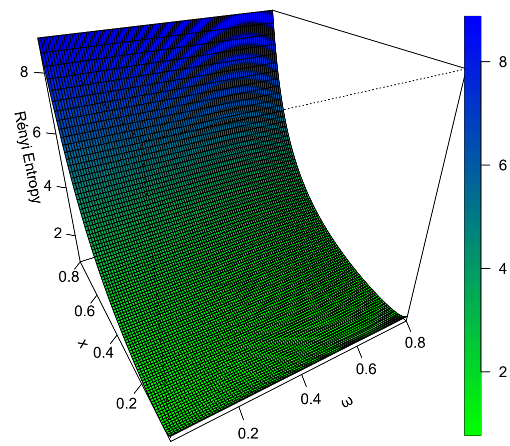

Figure 12: Rény entropy of PXSD(θ, c)

Figure 11 is sufficient to advise a reliability engineer that potential harm to the system that assumes the proposed distribution should any stress act on it. As additional stress is exerted on it, the reliability takes a maximum of zero, that is $-\infty\leq R_E\leq 0$. Figure 12 shows that $10\times\omega$ randomness exists in the system.

4 Non-Bayesian Estimation

In this section, we discuss two classical approaches to parameter estimation namely the maximum likelihood and the maximum product spacing.

4.1 Maximum Likelihood Estimation

Estimating the parameters of the PXSD is important in studying the behavior of the model. The maximum likelihood appears more applicable in the literature among other classical methods of estimation. Let $(y_1, y_2, \cdots, y_n)$ random samples of size n with joint PDF $f(y_1, y_2, \cdots, y_n;\theta, c)$. The likelihood function can be expressed as

$$L(y_1,y_2,\cdots,x_n;\theta,c)\propto\prod_{i=1}^{n}f(y_1,y_2,\cdots,y_n;\theta,c)=\frac{c^n\theta^{2n}}{\left(\theta^2+1\right)^{2n}}e^{-\theta\sum_{i=0}^{n}y^c}\prod_{i=1}^{n}\left(\theta^3+2\theta+y^c\right)y^{c-1} \tag{27}$$

Taking the natural logarithm will lead to

$$\ell=n\ln c+2n\ln\theta-2n\ln\left(\theta^2+1\right)-\theta\sum_{i=1}^{n}y^c+\sum_{i=1}^{n}\ln\left(\theta^3+2\theta+y^c\right)+(c-1)\sum_{0}^{n}\ln y \tag{28}$$

The maximum values of $\hat{\theta}$ and $\hat{c}$ are obtained by differentiating partially with respect to θ and c. That is,

$$\frac{\partial\ell}{\partial\theta}=\frac{2n}{\theta}-\frac{4n\theta}{\theta^2+1}-\sum_{i=1}^{n}y^c+\sum_{i=1}^{n}\frac{3\theta^2+2}{\theta^3+2\theta+y^c}+\sum_{i=1}^{n}\ln y \tag{29}$$

and

$$\frac{\partial\ell}{\partial c}=\frac{n}{c}-\theta\sum_{i=1}^{n}y^c\ln y+\sum_{i=1}^{n}\frac{y^c\ln y}{\theta^3+2\theta+y^c}+\sum_{i=1}^{n}\ln y \tag{30}$$

The two derivatives are not compact, meaning that their solutions are found through numerical iteration. This can be implemented in *R*.

4.2 Maximum Product Spacing Estimation

Consider the data to be in ascending order at this point, the PXSD greatest product spacing is given as

$$G_{i:m:n}(\theta, c \mid y_i) = \left(\prod_{i=1}^{n+1} D_i(y_i, \theta, c)\right)^{\frac{1}{n+1}} \tag{31}$$

Where $D_i(y_i, \theta, c) = F(y_i; \theta, c) - F(y_{i-1}; \theta, c), \quad i = 1, 2, \cdots, n$. In a like manner, one may decide to increase the function

$$S(\theta, c) = \frac{1}{n+1} \sum_{i=1}^{n+1} \ln D_i(\theta, c) \tag{32}$$

The parameter estimates are determined by solving the first derivative of the function $S(\xi)$ with respect to $\theta$and$c$ and solving the non-linear equations at $\frac{\partial S(\xi)}{\partial \theta} = 0$ and $\frac{\partial S(\xi)}{\partial c} = 0$ where $\xi = (\theta, c)$.

4.3 Least Squares Estimation

From Swain, Venkatraman, and Wilson (1988), we can derive the LSEs of the parameters θ and c as follows;

$$E[F(y_{i:n}|\theta, c)] = \frac{i}{n+1}; \quad V[F(y_{i:n}|\theta, c)] = \frac{i(n-i+1)}{(n+1)^2(n+2)}.$$

Minimize the function $L(\theta, c)$ to obtain the estimates $\hat{\theta}_{LSE}$ and $\hat{c}_{LSE}$ of the parameters θ and c as follows

$$L(\theta, c) = \underset{(\theta, c)}{\arg\min} \sum_{i=1}^{n} \left[F(y_{i:n}|\theta, c) - \frac{i}{n+1}\right]^2. \tag{33}$$

Resolving the following non-linear systems of equations produces the estimates

$$\sum_{i=1}^{n} \left[F(y_{i:n}|\theta, c) - \frac{i}{n+1}\right]^2 \Delta_1(y_{i:n}|\theta, c) = 0 \tag{34}$$

$$\sum_{i=1}^{n} \left[F(y_{i:n}|\theta, c) - \frac{i}{n+1}\right]^2 \Delta_2(y_{i:n}|\theta, c) = 0 \tag{35}$$

where

$$\Delta_1(y_{i:n}|\theta, c) = \frac{\left(\theta^2+1\right)^4 - \left(\theta^2+1\right)\left[\left(\theta^2+1\right)\left(1-\theta y^c\right) - 4\theta^2\right]}{\left(\theta^2+1\right)^4}. \tag{36}$$

$$\Delta_2(x_{i:n}|\theta, c) = \frac{\left(\theta^2+1\right)^2 + \theta y^c - 1}{\left(\theta^2+1\right)^2}. \tag{37}$$

4.4 Weighted Least Squares Estimation

Minimize the function $W(\theta, c)$ to obtain the estimates $\hat{\theta}_{WLSE}$ and $\hat{c}_{WLSE}$ of the proposed PXSD parameters θ and c as follows

$$W(\theta, c) = \underset{(\theta, c)}{\arg\min} \sum_{i=1}^{n} \frac{(n+1)^2(n+2)}{i(n-i+1)} \left[F(y_{i:n}|\theta, c) - \frac{i}{n+1}\right]^2. \tag{38}$$

Resolving the following non-linear systems of equations produces the estimates

$$\sum_{i=1}^{n}\frac{(n+1)^2(n+2)}{i(n-i+1)}\left[F(y_{i:n}|\theta,c)-\frac{i}{n+1}\right]\Delta_1(y_{i:n}|\theta,c)=0 \tag{39}$$

$$\sum_{i=1}^{n}\frac{(n+1)^2(n+2)}{i(n-i+1)}\left[F(y_{i:n}|\theta,c)-\frac{i}{n+1}\right]\Delta_2(y_{i:n}|\theta,c)=0, \tag{40}$$

$\Delta_1(y.|\theta,c)$ and $\Delta_2(y.|\theta,c)$ are respectively defined in (36) and (37).

4.5 Cramér-von-Mises Estimation

We minimize the function $C(\theta, c)$ to obtain the estimates $\hat{\theta}_{CVME}$, and $\hat{c}_{CVME}$ of the PXSD parameters θ, and c as follows

$$C(\theta,c)=\underset{(\theta,c)}{\arg\min}\left\{\frac{1}{12n}+\sum_{i=1}^{n}\left[F(y_{i:n}|\theta,c)-\frac{2i-1}{2n}\right]^2\right\}. \tag{41}$$

Resolving the following non-linear systems of equations produces the estimates

$$\left.\begin{aligned}\sum_{i=1}^{n}\left(F(y_{i:n}|\theta,c)-\frac{2i-1}{2n}\right)\Delta_1(y_{i:n}|\theta,c)=0\\ \sum_{i=1}^{n}\left(F(y_{i:n}|\theta,c)-\frac{2i-1}{2n}\right)\Delta_2(y_{i:n}|\theta,c)=0,\end{aligned}\right\} \tag{42}$$

$\Delta_1(y.|\theta,c)$ and $\Delta_2(y.|\theta,c)$ are respectively defined in (36) and (37).

4.6 Anderson-Darling Estimation

We minimize the function $A(\theta,c)$ to obtain the estimates $\hat{\theta}_{ADE}$, and $\hat{c}_{ADE}$ of the PXSD parameters θ and c as follows

$$A(\theta,c)=\underset{(\theta,c)}{\arg\min}\sum_{i=1}^{n}(2i-1)\left\{\ln F(y_{i:n}|\theta,c)+\ln\left[1-F(y_{n+1-i:n}|\theta,c)\right]\right\}. \tag{43}$$

Resolving the following non-linear systems of equations produces the estimates

$$\left.\begin{aligned}\sum_{i=1}^{n}(2i-1)\left[\frac{\Delta_1(y_{i:n}|\theta,c)}{F(y_{i:n}|\theta,c)}-\frac{\Delta_1(y_{n+1-i:n}|\theta,c)}{1-F(y_{n+1-i:n}|\theta,c)}\right]=0\\ \sum_{i=1}^{n}(2i-1)\left[\frac{\Delta_2(y_{i:n}|\theta,c)}{F(y_{i:n}|\theta,c)}-\frac{\Delta_2(y_{n+1-i:n}|\theta,c)}{1-F(y_{n+1-i:n}|\theta,c)}\right]=0,\end{aligned}\right\} \tag{44}$$

where $\Delta_1(y.|\theta,c)$ and $\Delta_2(y.|\theta,c)$ is as defined in (36) and (37) respectively.

4.7 Right-tailed Anderson-Darling Estimation

We minimize the function $R(\theta,c)$ to obtain the estimates $\hat{\theta}_{RTADE}$ and $\hat{c}_{RTADE}$ of the PXSD parameters θ and c as follows

$$R(\theta,c)=\underset{(\theta,c)}{\arg\min}\left\{\frac{n}{2}-2\sum_{i=1}^{n}F(y_{i:n}|\theta,c)-\frac{1}{n}\sum_{i=1}^{n}(2i-1)\ln\left[1-F(y_{n+1-i:n}|\theta,c)\right]\right\}. \tag{45}$$

Resolving the following non-linear systems of equations produces the estimates

$$\left.\begin{aligned}-2\sum_{i=1}^{n}\frac{\Delta_1(y_{i:n}|\theta,c)}{F(x_{i:n}|\theta,c)}+\frac{1}{n}\sum_{i=1}^{n}(2i-1)\left[\frac{\Delta_1(y_{n+1-i:n}|\theta,c)}{1-F(y_{n+1-i:n}|\theta,c)}\right]=0\\ -2\sum_{i=1}^{n}\frac{\Delta_2(y_{i:n}|\theta,c)}{F(y_{i:n}|\theta,c)}+\frac{1}{n}\sum_{i=1}^{n}(2i-1)\left[\frac{\Delta_2(y_{n+1-i:n}|\theta,c)}{1-F(y_{n+1-i:n}|\theta,c)}\right]=0,\end{aligned}\right\} \tag{46}$$

$\Delta_1(y.|\theta,c)$ and $\Delta_2(y.|\theta,c)$ are respectively defined in (36) and (37).

5 Bayesian Estimation

For tests with limited sample sizes or when there is censored data present, classical approaches can occasionally generate erroneous and misleading results. To provide more explicit estimates in this situation, the Bayesian approach could make use of more prior knowledge, such as historical data or an understanding of the statistical inferential process. In this section, we obtain Bayesian estimates that take parameter uncertainties into account and deal with the parameters as random variables. The joint prior distribution is used to define the knowledge of the parameter uncertainties before the gathering of failure data. Because it allows for the addition of prior information in the analysis, the Bayesian approach is very helpful in reliability analysis. This is significant because the lack of readily available data is one of the major hassles with reliability research. The unknown parameter θ, c is estimated using the Bayesian estimation (BE) technique under the assumption that its prior distribution is uninformative. Also, applying gamma prior for the variables θ and c with pdfs in the parameter prior distribution of PXSD.

$$\begin{aligned}\pi_1(\theta) &\propto \theta^{k_1-1}e^{-t_1\theta}; \quad \theta>0, \quad k_1>0, \quad t_1>0\\ \pi(c) &\propto c^{k_2-1}e^{-t_2 c}; \quad c>0, \quad k_2>0, \quad t_2>0\end{aligned} \tag{47}$$

Where the hyperparameter $k_s, t_s, s=1,2$ are selected to reject the prior knowledge about the unknown parameter. The joint prior for $\omega=(\theta,c)$ is given by

$$\begin{aligned}\pi(\omega) &= \pi_1(\theta)\pi_2(c)\\ \pi(\omega) &\propto \theta^{k_1-1}c^{k_2-1}e^{\{-t_1\theta-t_2c\}}\end{aligned} \tag{48}$$

The corresponding posterior distribution density given the observed data $y=(y_1,y_2,\ldots,y_n)$ is given by

$$\pi(\omega\mid\mathbf{y}) = \frac{\pi(\omega)\ell(\omega)}{\int_\omega \pi(\omega)\ell(\omega)d\omega}$$

Consequently, the posterior density function is given by

$$\pi(\omega\mid\mathbf{y}) \propto \frac{c^{n+k_2-1}\theta^{2n+k_1+-1}}{\left(\theta^2+1\right)^{2n}}e^{-(t_1\theta-t_2c)-\theta\sum_{i=1}^{n}y_i^c}\prod_{i=1}^{n}\left(\theta^3+2\theta+y_i^c\right)y_i^{c-1} \tag{49}$$

Given any function, such as $l(\omega)$ under the squared error loss (SEL) function, the Bayes estimator is given as

$$\hat{\omega}_{BE_{SEL}} = E[l(\omega)\mid\mathbf{y}] = \int_\omega l(\omega)\pi(\omega\mid y)d\omega \tag{50}$$

The SEL being a symmetrical loss function regards overestimation and underestimation equally. In real-life situations, both overestimation and underestimation can have serious implications. The linear exponential loss function (LINEX) can be used in certain instances as an alternative to the SEL function given by

$$(l(\omega),\hat{l}(\omega)) = e^{\{\hat{l}(\omega)-l(\omega)\}} - \tau(\hat{l}(\omega)-l(\omega))-1$$

Where $\tau\neq 0$ is a shape parameter. Here, $\tau>1$ insinuates that an overestimation is more serious than an underestimation and vice-versa for $\tau>0$. Further, as τ approaches zero it replicates the SE loss function. For more details in this regard, one should refer to Varian (1975) and Doostparast, Akbari, and Balakrishna (2011). The BE of $l(\omega)$ under this loss function is given by

$$\omega_{BE_{LINEX}} = E[e^{\{-\tau(\omega)\}}\mid\mathbf{y}] = -\frac{1}{\tau}\log\left[\int_\omega e^{\{-\tau(\omega)\}}\pi(\omega\mid y)d\omega\right] \tag{51}$$

Likewise, we consider the general entropy loss(GEL) suggested by Calabria and Pulcini (1996) defined as

$$(l(\omega),\hat{l}(\omega) = \left(\frac{\hat{l}(\omega)}{l(\omega)}\right)^\nu - \nu\log\left(\frac{\hat{(\omega)}}{l(\omega)}\right)-1$$

Where $\nu\neq 0$ denotes a divergence from symmetry. It views overestimation as more significant than underestimation when $\nu>0$ and vice-versa when $\nu<0$.The Bayes estimator of $l(\omega)$ under the GE loss function is as follows

$$\omega_{BE_{GEL}} = \left[E((l(\omega))^{-\nu}\mid y)\right]^{\frac{-1}{\nu}} = \left[\int_\omega (l(\omega))^{-\nu}\pi(\omega\mid y)d\omega\right]^{-\frac{1}{\nu}} \tag{52}$$

Where there is no analytical solution to the computation of equation 50, 51 and 52, the Markov chain Monte Carlo (MCMC) approach to generate posterior samples and arrive at suitable BEs is then used. It is possible to properly quantify the posterior uncertainty with respect to the parameter ω using a kernel estimate of the posterior distribution and the MCMC samples.

Lastly, part of the initial samples can be eliminated (burn-in) from the random samples of size M derived from the posterior density, and the remaining samples can then be used to calculate Bayes estimates. Using MCMC under the SEL, LINEX, and GEL functions, the BEs of ωi = (θ)i,(c)i can be calculated as

$$\hat{\omega}_{BE_{SEL}} = \frac{1}{M-l_B}\sum_{i=l_B}^{M}\omega^{(i)} \tag{53}$$

$$\hat{\omega}_{BE_{LINEX}} = -\frac{1}{\tau}\log\left[\frac{1}{M-l_B}\sum_{i=l_B}^{M}e^{\{-\tau\omega^{(i)}\}}\right] \tag{54}$$

$$\hat{\omega}_{BE_{GEL}} = \left[\frac{1}{M-l_B}\sum_{i=l_B}^{M}\left(\omega^{(i)}\right)^{-\nu}\right]^{\frac{-1}{\nu}} \tag{55}$$

where l_B represents the number of burn-in samples.

5.1 Credible intervals for Bayes estimates

A $100(1-\gamma)\%$ credible intervals for the parameters $\phi = (\theta, c)$ under the loss functions discussed are

$$\hat{\phi}_{BE_{SEL}} \pm Z_{\frac{\gamma}{2}}\sqrt{var(\hat{\phi}_{BE_{SEL}})};\quad \hat{\phi}_{BE_{LINEX}} \pm Z_{\frac{\gamma}{2}}\sqrt{var(\hat{\phi}_{BE_{LINEX}})};\quad \hat{\phi}_{BE_{GEL}} \pm Z_{\frac{\gamma}{2}}\sqrt{var(\hat{\phi}_{BE_{GEL}})} \tag{56}$$

where $Z_{\frac{\gamma}{2}}$ is distributed according to percentile standard normal with right-tailed probability.

6 Simulation Study

In this section, we simulate data for the PXSD to show how good each of the non-Bayesian estimation methods is. First, 1000 data points are generated from the PXSD by considering the initial parameter values as

- θ = 0.50 and c = 2.0
- θ = 0.5 and c = 1.5

and sample sizes n = 50,100,150,200. For each estimate ˆφ = (ˆθ , ˆ c), the Bias and Root Mean Squared Error (RMSE) are calculated respectively as

$$Bias(\hat{\phi}) = \frac{1}{N}\sum_{i=1}^{N}(\hat{\phi}_i - \phi), \quad \text{and} \quad RMSE(\hat{\phi}) = \sqrt{\frac{1}{N}\sum_{i=1}^{N}(\hat{\phi}_i - \phi)^2}.$$

To locate the desired estimates for the Non-Bayesian process, we employed the Newton-Raphson algorithm. With the Bayesian approach, BEs are generated while accounting for prior knowledge using MCMC and the MH algorithm. We made the gamma distribution hyper-parameters for the prior data equal to double the parameter values. These values were filled in to provide the estimates we were looking for. The maximum likelihood estimates consider initial guess values by using the MH method. To acquire the Bayes estimates under SEL, LINEX at $\nu = -1.5, 1.5$, and the GEL at $\tau = -0.5, 0.5$, we finally eliminate 2000 burn-in samples from the overall 10000 samples produced from the posterior density. We calculate the bias and RMSE for each strategy. For the MCMC method, there are two types of graphs: marginal posterior and cumulative sum plots for lambda and theta. The MCMC is a reliable method that, after a 5,000 burn-in from a 10,000 sample draw, meets stability and convergences.

Table 1: Average estimated Biases and RMSEs of various estimation techniques for the PXSD for various sample sizes n and various parameter values ($\theta = 0.50$, $c = 2.0$).

Method		$n = 50$		$n = 100$		$n = 150$		$n = 200$	
		Bias	RMSE	Bias	RMSE	Bias	RMSE	Bias	RMSE
ML	θ	0.06664	0.00457	0.06696	0.00454	0.06664	0.00448	0.06625	0.00442
	c	0.00428	0.01785	0.00964	0.00910	0.01557	0.00620	0.01372	0.00417
MPS	θ	0.01664	0.00429	0.00693	0.00202	0.00511	0.00136	0.00537	0.00102
	c	0.06944	0.03696	0.03898	0.01642	0.03182	0.01133	0.02614	0.00850
LE	θ	0.26430	0.08995	0.25255	0.07913	0.24507	0.07236	0.24013	0.06896
	c	0.00780	0.03760	0.00462	0.01817	0.00535	0.01315	0.00023	0.00867
WLS	θ	0.00157	0.00440	0.00290	0.00211	0.00222	0.00142	0.00068	0.00103
	c	0.01077	0.04340	0.01158	0.01857	0.00632	0.01237	0.00594	0.00950
CVM	θ	0.00449	0.00497	0.00568	0.00232	0.00380	0.00156	0.00168	0.00114
	c	0.04968	0.05940	0.02835	0.02413	0.01614	0.01604	0.01241	0.01234
AD	θ	0.00092	0.00431	0.00269	0.00208	0.00199	0.00141	0.00048	0.00103
	c	0.01493	0.03982	0.01124	0.01780	0.00539	0.01206	0.00513	0.00929
RTAD	θ	0.00102	0.00509	0.00444	0.00239	0.00325	0.00173	0.00113	0.00120
	c	0.02326	0.04608	0.01832	0.02028	0.01039	0.01423	0.00768	0.01020
BE_{SEL}	θ	0.07134	0.00537	0.07485	0.00569	0.07596	0.00582	0.07653	0.00589
	c	0.14448	0.03689	0.15458	0.03131	0.15816	0.02954	0.15999	0.02885
BE_{Linex1}	θ	0.07078	0.00529	0.07456	0.00565	0.07577	0.00579	0.07638	0.00587
	c	0.15135	0.03907	0.15811	0.03245	0.16054	0.03031	0.16178	0.02944
BE_{Linex2}	θ	0.07189	0.00544	0.07514	0.00573	0.07616	0.00585	0.07668	0.00591
	c	0.13762	0.03481	0.15104	0.03019	0.15578	0.02878	0.15820	0.02828
BE_{GEL1}	θ	0.07263	0.00555	0.07552	0.00579	0.07642	0.00589	0.07688	0.00594
	c	0.14127	0.03595	0.15293	0.03080	0.15706	0.02919	0.15916	0.02859
BE_{GEL2}	θ	0.07521	0.00593	0.07688	0.00600	0.07734	0.00603	0.07757	0.00605
	c	0.13483	0.03414	0.14964	0.02979	0.15485	0.02849	0.15750	0.02806

Table 2: Average estimated Biases and RMSEs of various estimation techniques for the PXSD for various sample sizes n and various parameter values (θ = 0.50, c = 1.5).

Method		$n = 50$		$n = 100$		$n = 150$		$n = 200$	
		Bias	RMSE	Bias	RMSE	Bias	RMSE	Bias	RMSE
ML	θ	0.06448	0.00430	0.06444	0.00422	0.06416	0.00417	0.06375	0.00410
	c	0.00097	0.01090	0.01164	0.00535	0.01404	0.00350	0.01600	0.00275
MPS	θ	0.01650	0.00442	0.00747	0.00218	0.00488	0.00149	0.00581	0.00102
	c	0.05123	0.02107	0.03084	0.00952	0.02155	0.00654	0.02240	0.00479
LS	θ	0.18492	0.04498	0.17521	0.03810	0.16747	0.03543	0.16663	0.03427
	c	0.00357	0.02235	0.00385	0.01072	0.00190	0.00744	0.00224	0.00510
WLS	θ	0.00140	0.00453	0.00226	0.00220	0.00269	0.00153	0.00021	0.00104
	c	0.00732	0.02466	0.00684	0.01064	0.00872	0.00756	0.00094	0.00532
CVM	θ	0.00494	0.00499	0.00519	0.00238	0.00435	0.00166	0.00131	0.00114
	c	0.03507	0.03230	0.01944	0.01373	0.01637	0.00986	0.00567	0.00683
AD	θ	0.00074	0.00442	0.00227	0.00217	0.00245	0.00151	0.00002	0.00104
	c	0.01042	0.02252	0.00713	0.01013	0.00786	0.00731	0.00017	0.00523
RTAD	θ	0.00350	0.00507	0.00421	0.00244	0.00336	0.00173	0.00114	0.00119
	c	0.02340	0.02673	0.01284	0.01110	0.01053	0.00796	0.00351	0.00573
BE_{SEL}	θ	0.07132	0.00539	0.07410	0.00559	0.07489	0.00566	0.07536	0.00572
	c	0.11380	0.02196	0.11779	0.01800	0.11917	0.01671	0.11998	0.01621
BE_{Linex1}	θ	0.07075	0.00531	0.07380	0.00554	0.07469	0.00563	0.07521	0.00569
	c	0.11778	0.02295	0.11983	0.01850	0.12055	0.01704	0.12101	0.01646
BE_{Linex2}	θ	0.07188	0.00547	0.07439	0.00563	0.07509	0.00569	0.07551	0.00574
	c	0.10982	0.02101	0.11575	0.01751	0.11779	0.01637	0.11894	0.01596
BE_{GEL1}	θ	0.07264	0.00557	0.07479	0.00569	0.07536	0.00573	0.07572	0.00577
	c	0.11132	0.02139	0.11652	0.01770	0.11832	0.01650	0.11934	0.01605
BE_{GEL2}	θ	0.07528	0.00596	0.07617	0.00590	0.07631	0.00588	0.07643	0.00588
	c	0.10636	0.02029	0.11399	0.01711	0.11661	0.01610	0.11806	0.01575

Table 3: Confidence Intervals for MLEs and Credible Intervals for the Bayesian Estimates using BE_{SEL}, BE_{Linex1}, BE_{Linex2}, BE_{GEL1} & BE_{GEL2}

Initial Value	lower ML	Upper ML	Lower BE_{SEL}	Upper BE_{SEL}	Lower BE_{Linex1}	Upper BE_{Linex1}	Lower BE_{Linex2}	Upper BE_{Linex2}	Lower BE_{GEL1}	Upper BE_{GEL1}	Lower BE_{GEL2}	Upper BE_{GEL2}
$\theta = 0.5$	0.39261	0.46001	0.06740	0.40576	0.44223	0.03648	0.40943	0.43689	0.02746	0.41265	0.43464	0.02199
$c = 2.0$	1.87941	2.36974	0.49033	1.98911	2.32258	0.33348	2.02758	2.29585	0.26827	2.04376	2.26795	0.22419
$\theta = 0.5$	0.39267	0.46269	0.07002	0.40566	0.44419	0.03853	0.40996	0.43898	0.02902	0.41315	0.43648	0.02333
$c = 1.5$	1.41986	1.79077	0.37091	1.49454	1.74489	0.25035	1.52351	1.72418	0.20067	1.54256	1.71013	0.16757

The simulation study's Tables (1-2) allow for the following deductions.

- The results of Tables (1-2) show the stability of the PXSD because the Bias and RMSE for the parameters of the PXSD are relatively small.
- As the sample size increases, we occasionally observe a decrease in the Bias and RMSE for all estimations.
- This indicates that using a variety of estimation techniques yields reliable Bias and RMSE results for big sample sizes.
- The WLS estimation method offers better metrics than the ML, MPS, LS, CVM, AD, and RTAD approaches.
- All estimators' Bias and RMSE values decrease as sample size rises, indicating improved model parameter estimation accuracy.
- All sample sizes have a positive estimators' bias.
- From Tables (1-2), we noted that the WLS, LS, CVM, AD, RTAD, ML, and Bayesian methods respectively, give smaller values for accurate Bias and RMSE findings for large sample sizes.

7 Applications

The first data consists of thirty successive values of March precipitation (in inches) in Minneapolis/St Paul from Hinkley (1977) and studied by EL-Helbawy, AL-Dayian, and Abd AL-Fattah (2020).

Table 4: Thirty successive values of March precipitation (in inches) in Minneapolis/St Paul

0.77	1.74	0.81	1.20	1.95	1.2	0.47	1.43	3.37	2.2
3.0	3.09	1.51	2.1	0.52	1.62	1.31	0.32	0.59	0.81
2.81	1.87	1.18	1.35	4.75	2.48	0.96	1.89	0.9	2.05

Table 5: Goodness of fit measures and performance indices for data I

Dist.	NLL	CVM	AD	AIC	CAIC	BIC	HQIC	P-value
PXSD	43.04	0.0172	0.1347	90.0861	90.5306	92.8885	90.9826	0.718
PP	44.46	0.1960	1.1618	92.9191	93.3635	95.7215	93.8156	0.5807
Shanker	42.99	0.0144	0.1126	87.9748	88.1176	89.3760	88.4230	0.3216
TPRD	40.51	0.0281	0.2275	85.0114	85.4558	87.8137	85.9079	0.8170
Lindley	43.14	0.0144	0.1123	88.2875	88.4303	89.6886	88.7357	0.2384
xgamma	44.57	0.0189	0.1446	91.1471	91.2899	92.5483	91.5953	0.1021

The competing distribution fitted on the data sets are Power Prakaamy distribution by Shukla and Rama Shanker (2020), Shanker distribution by Shanker (2015), two-parameter Rani distribution by Al-Omari, Aidi, and Seddik-Ameur (2021), Lindley distribution by Lindley (1958) and Xgamma distribution by Sen, Maiti, and Chandra (2016). The following statistics were computed for the model performance Negative Log-Likelihood (NLL), cramér von Misses (CVM), Anderson-Darling (AD), Akaike Information Criterion (AIC), conditional AIC (cAIC), Bayesian Information Criterion (BIC), and the Hannan-Quinn information criterion (HQIC). The Kolmogorov-Smirnov statistic p-value is used as a model. adequacy measure.

Table 6: PXSD Parameter Estimates for data I using various methods

Method		θ	c
ML	Estimate	0.70249	1.25642
	Std. Error	0.10102	0.17077
MPS	Estimate	0.62434	1.43630
	Std. Error	0.09246	0.17530
LS	Estimate	0.61904	1.54419
	Std. Error	0.26108	1.04752
WLS	Estimate	0.61255	1.54734
	Std. Error	0.01812	0.06550
CVM	Estimate	0.60655	1.61478
	Std. Error	0.26265	1.08422
AD	Estimate	0.60444	1.58580
	Std. Error	0.10559	0.34951
RTAD	Estimate	0.62851	1.50989
	Std. Error	0.18324	0.49830
BE	Estimate	0.67927	1.31921
	Std. Error	0.08313	0.05845

The WLS method has the least standard error in estimating θ while BE has the smallest standard error in estimating c. Relatively, WLS and the BE are the best methods for estimating the parameters of PXSD using the first data.

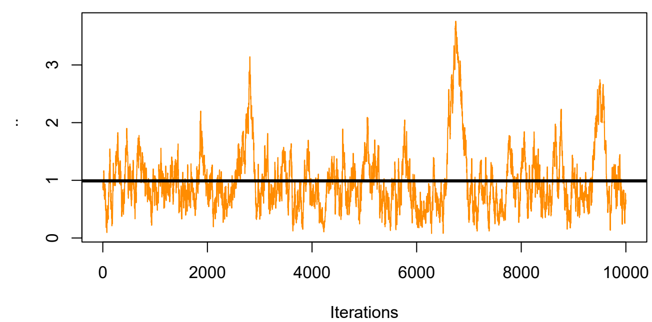

Figure 13: MCMC trace for θ using data I

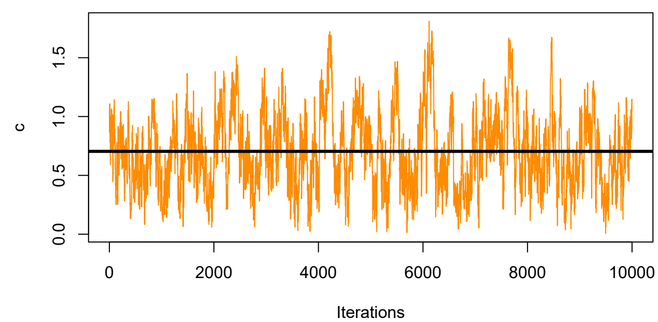

Figure 14: MCMC trace for c using data I

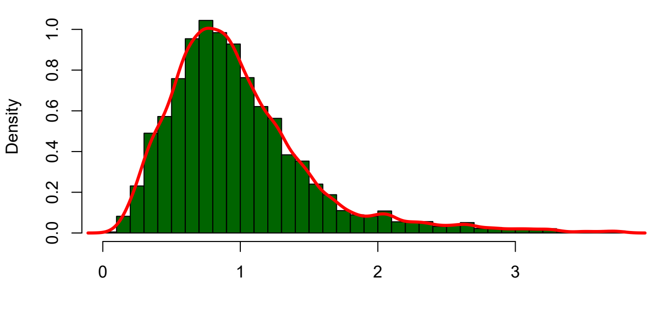

Figure 15: posterior density for θ using data I

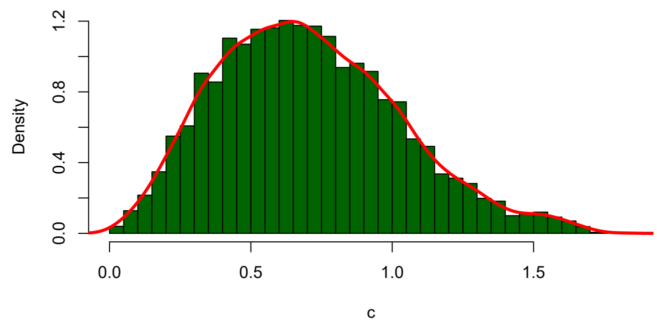

Figure 16: posterior density for c using data I

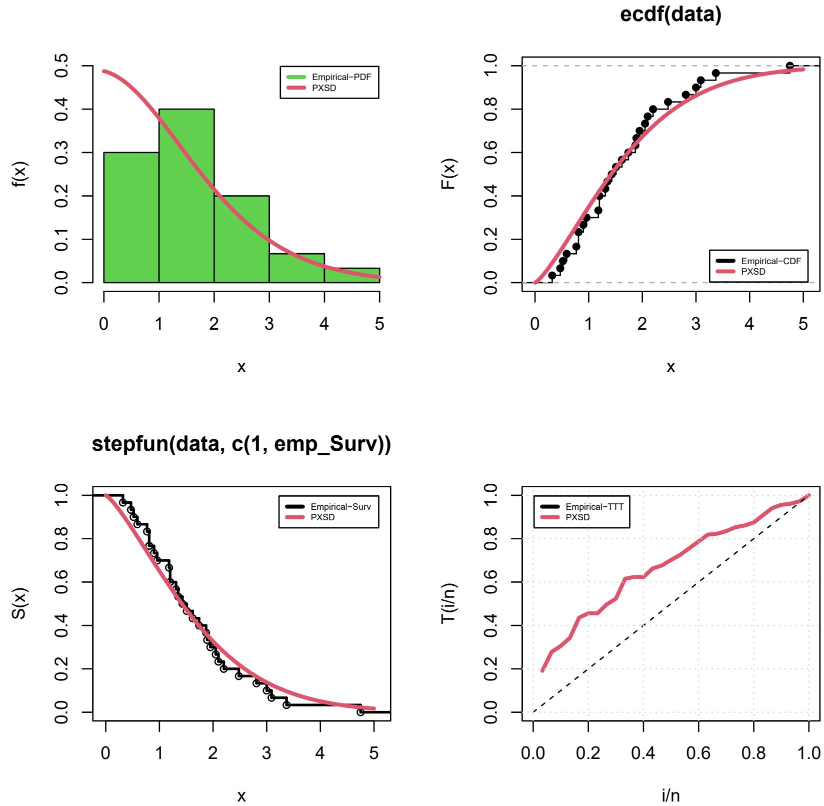

Figure 17: Density, CDF, Survival function and TTT plots for data I

From figure 17, it is clear that the model approximates the empirical lines. This reflects better goodness of fit in the first data scenario.

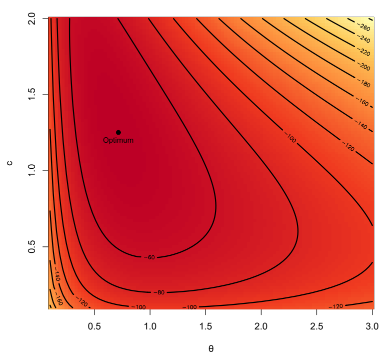

Figure 18: Contour of log-likelihood for data I

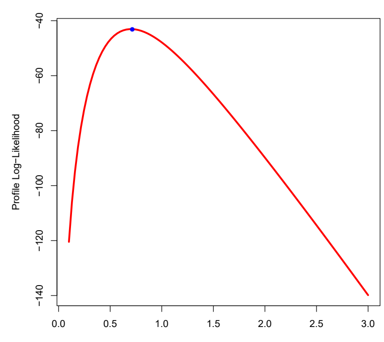

Figure 19: profile log-likelihood for θ using data I

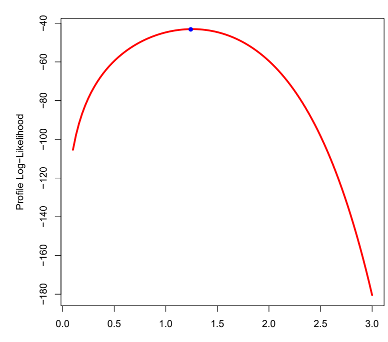

Figure 20: profile log-likelihood for c using data I

The second application is on the total factor productivity (TFP) growth agricultural production for thirty-seven African countries from 2001-2010 studied by MOAKOF˙I and OLUYEDE (2023).

Table 7: Total factor productivity (TFP) growth agricultural production for thirty-seven African countries from 2001-2010

4.6	0.9	1.8	1.4	0.2	3.9	1.8	0.8	2.0	0.8	1.6	0.8	2.0
1.6	0.5	0.1	2.5	2.4	0.6	1.1	0.7	1.7	1.0	1.7	2.5	3.5
0.3	0.9	2.3	0.5	1.5	5.1	0.2	1.5	3.3	1.4	3.3		

Table 8: Goodness of fit measures and performance indices for data II

Dist.	NLL	CVM	AD	AIC	CAIC	BIC	HQIC	P-value
PXSD	55.15	0.0291	0.1767	114.6511	114.2982	117.52	115.434	0.8044
PP	58.11	0.1992	1.1144	120.2268	120.5798	123.4486	121.3627	0.4171
Shanker	54.75	0.0290	0.1790	111.4963	111.6105	113.1072	112.0642	0.7229
TPRD	56.04	0.1079	0.6715	116.0767	116.4296	119.2985	117.2125	0.7032
Lindley	54.85	0.0291	0.1795	111.6938	111.8081	113.3047	112.2617	0.6352
xgamma	55.69	0.0318	0.1961	113.3826	113.4969	114.9936	113.9506	0.4620

In the second data scenario, the metrics of model fitness (K-S p-value) in table 8 show that the proposed PXSD better fits the data more than the competing distributions.

Table 9: PXSD Parameter estimates for data II using various methods

Methods		θ	c
ML	Estimate	0.74451	1.12480
	Std. Error	0.09509	0.13638
MPS	Estimate	0.72252	1.14087
	Std. Error	0.09229	0.13578
LS	Estimate	0.69683	1.24184
	Std. Error	0.24426	0.83060
WLS	Estimate	0.70173	1.21176
	Std. Error	0.01608	0.04497
CVM	Estimate	0.68758	1.29276
	Std. Error	0.24625	0.85999
AD	Estimate	0.69182	1.25862
	Std. Error	0.10020	0.26488
RTAD	Estimate	0.70043	1.23696
	Std. Error	0.17152	0.38419
BE	Estimate	0.68963	1.21984
	Std. Error	0.07036	0.03423

From table 9, it is also obvious that in estimating θ, the WLS has the least standard error for data II while the BE has the least for estimating the parameter c.

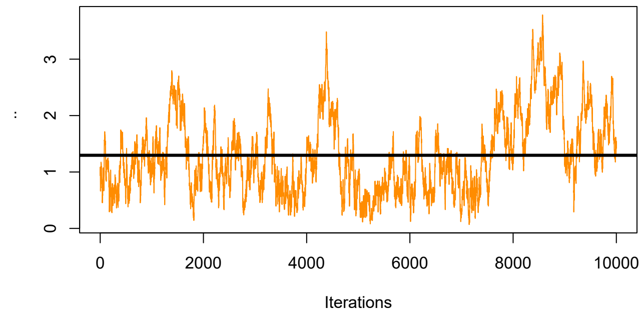

Figure 21: MCMC trace for θ using data II

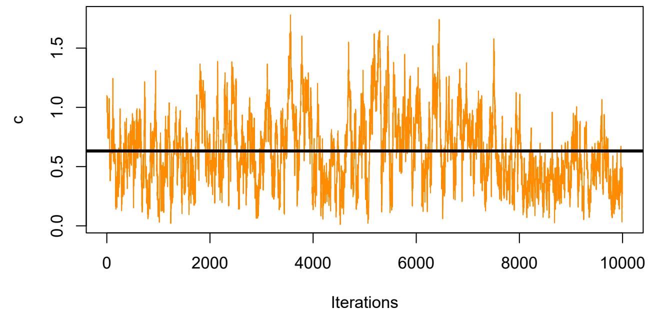

Figure 22: MCMC trace for c using data II

Figure 23: posterior density for θ using data II

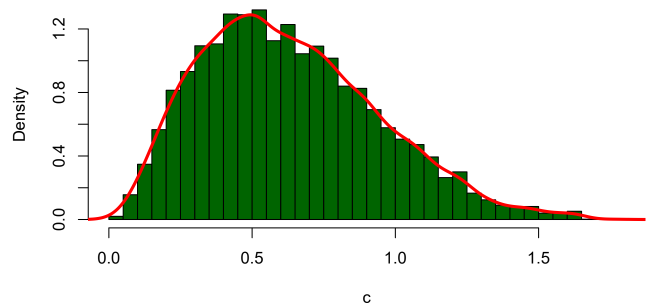

Figure 24: posterior density for c using data II

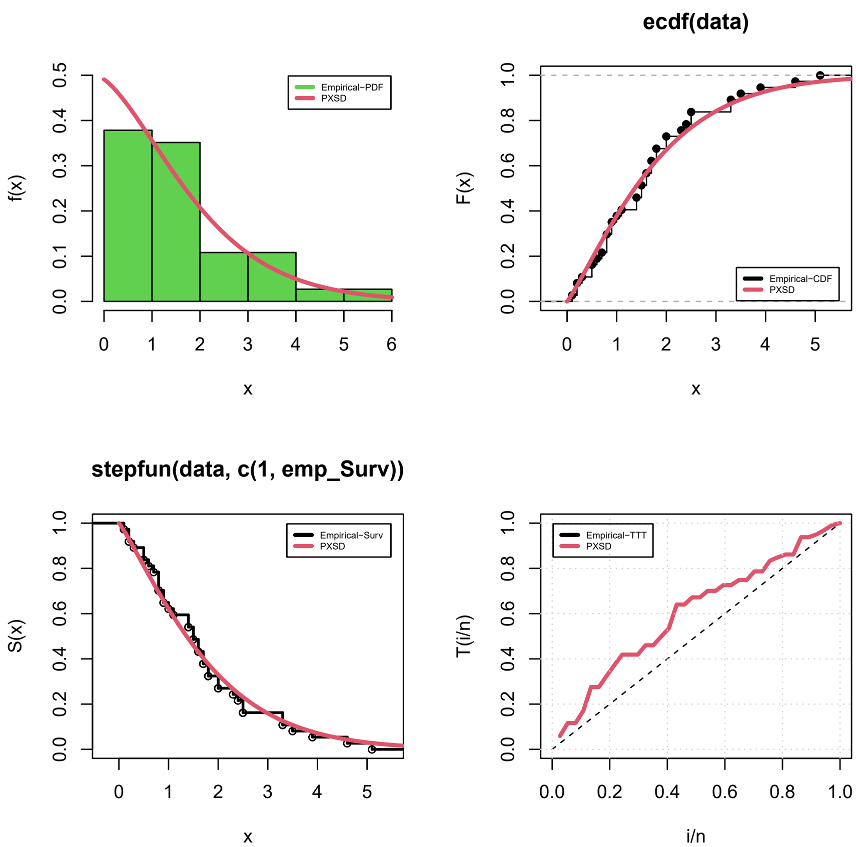

Figure 25: Density, CDF, Survival function and TTT plots for data II

The estimations clearly show that all of the generated posteriors are symmetric with respect to the theoretical posterior density functions. Figures 13 and 14 show the trace plots of the posterior distributions of the parameters to track the convergence of the MCMC outputs. This figure shows how well the MCMC process converges. The estimations clearly show that all of the generated posteriors are symmetric with respect to the theoretical posterior density functions. Using the log-likelihood function in the two data scenarios, the contour plots in figures 18 and 26 display the relationship between the two parameters of the PXSD model, and indicated in the two plots are the optimum points of the relationship.

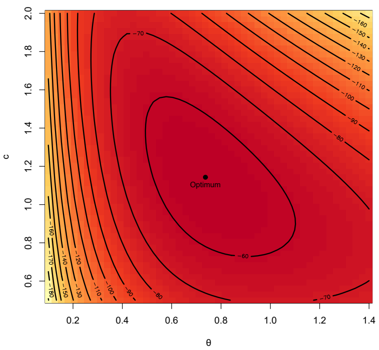

Figure 26: Contour of log-likelihood for data II

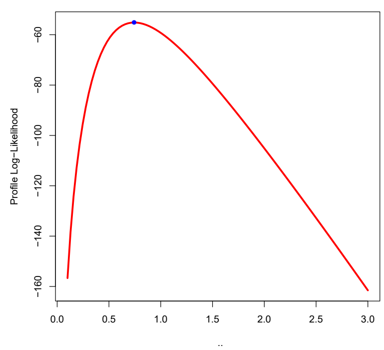

Figure 27: profile log-likelihood for θ using data II

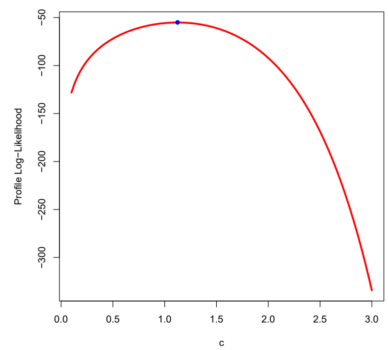

Figure 28: profile log-likelihood for c using data II

The profile log-likelihood plots in figures 19, 20, 27 and 28 support the exact estimates obtained for MLE in both data instances reflecting consistency.

8 Concluding Remarks

We have shown how well the proposed power XShanker distribution can model lifetime data. Essentially, this proposition is one among many Lindley class of distributions that possesses closed-form quantile functions thereby making it diverse in application and particularly aiding data generation. In addition, we showed the estimation of the parameters of the proposed model using the Bayesian method under squared error loss, linear-exponential loss, and generalized entropy loss functions. Illustrations of the Bayesian method potential are evident in the applications on precipitation and total factor productivity data sets. The Bayesian estimation procedure is better than the competing distributions in estimating the shape parameter of the model c.

References

1. Ezeilo, C. I., Umeh, E. U., Osuagwu, D. C., & Onyekwere, C. K. (2023). Exploring the impact of factors affecting the lifespan of HIVs/AIDS patient's Survival: An investigation using advanced statistical techniques. Open Journal of Statistics, 13(4), 595-619.
2. Ghitany, M. E., Al-Mutairi, D. K., Balakrishnan, N., & Al-Enezi, L. J. (2013). Power Lindley distribution and associated inference. Computational Statistics & Data Analysis, 64, 20-33.
3. Al-Omari, A. I., Alhyasat, K., Ibrahim, K., & Abu Bakar, M. A. (2019). Power length-biased Suja distribution: Properties and application. Electronic Journal of Applied Statistical Analysis, 12(2), 429-452.
4. Abdelall, Y. Y. (2023). New Odoma Distribution with Application to Cancer Data. Indian Journal of Science and Technology, 16(11), 839-849.
5. Abebe, B., Tesfay, M., Eyob, T., & Shanker, R. (2019). A two-parameter power Rama distribution with properties and applications. Biometrics and Biostatistics International Journal, 8(1), 6-11.
6. Shanker, R., & Shukla, K. K. (2017). Power Shanker distribution and its application. Türkiye Klinikleri Biyoistatistik, 9(3), 175-187.
7. Shukla, K. K., & Shanker, R. (2018). Power Ishita distribution and its application to model lifetime data. Statistics in Transition new series, 19(1).
8. Ikechukwu, A. F., Eghwerido, J. T., & Emmanuel, R. F. (2021). The type II topp-Leone generalized power Ishita distribution with properties and applications. Thailand Statistician, 19(3), 472-483.
9. Elnagar, K. A., Ramadan, D. A., & El-Desouky, B. S. (2022). Statistical Inference to the Parameter of the Inverse Power Ishita Distribution under Progressive Type-II Censored Data with Application to COVID-19 Data. Journal of Mathematics, 2022.
10. Ferreira, A. A., & Cordeiro, G. M. (2023). The exponentiated power Ishita distribution: Properties, simulations, regression, and applications. Chilean Journal of Statistics (ChJS), 14(1).
11. Shukla, K. K., & Shanker, R. (2020). Power Prakaamy distribution and its applications. International Journal of Computational and Theoretical Statistics, 7(01).
12. Obulezi, O. J., Ujunwa, O. E., Anabike, I. C., & Igbokwe, C. P. (2023). The Exponentiated Power Chris-Jerry Distribution: Properties, Regression, Simulation and Applications to Infant Mortality Rate and Lifetime of COVID-19 Patients. TWIST, 18(4), 328-337.
13. Etaga, H. O., Nwankwo, M. P., Oramulu, D. O., & Obulezi,

O. J. (2023). An Improved XShanker Distribution with Applications to Rainfall and Vinyl Chloride Data. Sch J Eng Tech, 9, 212-224.
14. Etaga, H. O., Celestine, E. C., Onyekwere, C. K., Omeje, I. L., Nwankwo, M. P., Oramulu, D. O., & Obulezi, O. J. (2023). A new modification of Shanker distribution with applications to increasing failure rate data. Earthline Journal of Mathematical Sciences, 13(2), 509-526.
15. Obulezi, O. J., Anabike, I. C., Okoye, G. C., Igbokwe, C. P., Etaga, H. O., & Onyekwere, C. K. The Kumaraswamy Chris-Jerry Distribution and its Applications.
16. Swain, J. J., Venkatraman, S., & Wilson, J. R. (1988). Least-squares estimation of distribution functions in Johnson's translation system. Journal of Statistical Computation and Simulation, 29(4), 271-297.
17. Varian, H. R. (1975). A Bayesian approach to real estate assessment. Studies in Bayesian econometrics and statistics in honor of Leonard J. Savage.
18. Doostparast, M., Akbari, M. G., & Balakrishna, N. (2011). Bayesian analysis for the two-parameter Pareto distribution based on record values and times. Journal of Statistical Computation and Simulation, 81(11), 1393-1403.
19. Calabria, R., & Pulcini, G. (1996). Point estimation under asymmetric loss functions for left-truncated exponential samples. Communications in Statistics-Theory and Methods, 25(3), 585-600.
20. Hinkley, D. (1977). On quick choice of power transformation. Journal of the Royal Statistical Society: Series C (Applied Statistics), 26(1), 67-69.
21. EL-Helbawy, A. A. A., AL-Dayian, G. R., & Abd AL-Fattah, A. M. (2020). Statistical inference for inverted Kumaraswamy distribution based on dual generalized order statistics. Pakistan Journal of Statistics and Operation Research, 649-660.
22. Shanker, R (2015). “Shanker distribution and its applications”. In: International journal of statistics and Applications 5.6, pages 338–348 (cited on page 16).
23. Al-Omari, A. I., Aidi, K., & Seddik-Ameur, N. (2021). A Two Parameters Rani Distribution: Estimation and Tests for Right Censoring Data with an Application. Pakistan Journal of Statistics and Operation Research, 1037-1049.
24. Lindley, D. V. (1958). Fiducial distributions and Bayes' theorem. Journal of the Royal Statistical Society. Series B (Methodological), 102-107.
25. Sen, S., Maiti, S. S., & Chandra, N. (2016). The xgamma distribution: statistical properties and application. Journal of Modern Applied Statistical Methods, 15(1), 38.
26. MOAKOFİ, T., & OLUYEDE, B. (2023). The type I heavy-tailed odd power generalized Weibull-G family of distributions with applications. Communications Faculty of Sciences University of Ankara Series A1 Mathematics and Statistics, 72(4), 921-958.